ACS APPLIED MATERIALS & INTERFACES

Research Article

www.acsami.org

Highly Bright Yellow-Green-Emitting $CuInS_2$ Colloidal Quantum Dots with Core/Shell/Shell Architecture for White Light-Emitting Diodes

Sang Hyun Park,[†,∥] Ara Hong,[†,‡,∥] Jong-Hoon Kim,[§] Heesun Yang,[§] Kwangyeol Lee,[‡] and Ho Seong Jang*[,†,⊥]

[†]Materials Architecturing Research Center, Korea Institute of Science and Technology, Hwarangno 14-gil 5, Seongbuk-gu, Seoul 136-791, Republic of Korea

[‡]Department of Chemistry, Korea University, Seoul 136-701, Republic of Korea

[§]Department of Materials Science and Engineering, Hongik University, Seoul 121-791, Republic of Korea

[⊥]Korea University of Science and Technology, Daejeon 305-350, Republic of Korea

Supporting Information

ABSTRACT: In this study, we report bright yellow-green-emitting $CuInS_2$ (CIS)-based quantum dots (QDs) and two-band white light-emitting diodes (LEDs) using them. To achieve high quantum efficiency (QE) of yellow-green-emitting CIS QDs, core/shell/shell strategy was introduced to high quality CIS cores (QE = 31.7%) synthesized by using metal−oleate precursors and 1-dodecanethiol. The CIS/ZnS/ZnS QDs showed a high QE of 80.0% and a peak wavelength of 559 nm under the excitation of 450 nm, which is well matched with dominant wavelength of blue LEDs. The formation of core/shell/shell structure was confirmed by X-ray diffraction, transmission electron microscopy, and inductively coupled plasma-optical emission spectroscopy analyses. Intense and broad yellow-green emission band of the CIS/ZnS/ZnS is beneficial for bright two-band white light. When the CIS/ZnS/ZnS was coated on the blue LEDs, the fabricated white LED showed bright natural white light (luminous efficacy (η_L) = 80.3 lm·W^{-1}, color rendering index (R_a) = 73, correlated color temperature (T_c) = 6140 K). The QD−white LED package showed a high light conversion efficiency of 72.6%. In addition, the CIS/ZnS/ZnS-converted white LED showed relatively stable white light against the variation of forward bias currents of 20−150 mA [color coordinates (x, y) = (0.3320−0.3207, 0.2997−0.2867), R_a = 70−72, T_c = 5497−6375 K].

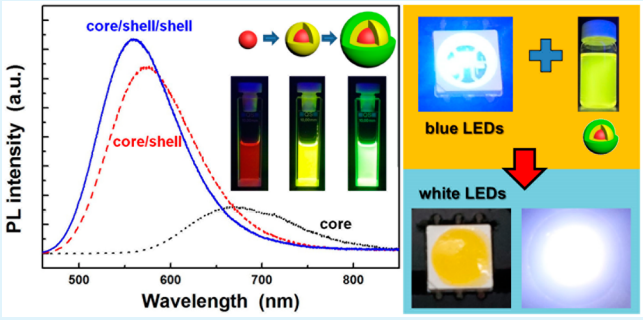

KEYWORDS: *core/shell/shell, luminescence, quantum dots, white LEDs*

1. INTRODUCTION

Colloidal semiconductor nanocrystals, so-called quantum dots (QDs), have been extensively studied for past three decades since the report on the synthesis of high quality colloidal CdE (E = S, Se, Te) in 1993.[1] Although many studies have reported CdSe-based QDs due to their high quantum efficiency (QE) and full color tunability from blue to red,[2] recently, Cd-free QDs are spotlighted because of toxicity issue.[3] For commercialization of QDs in optoelectronic devices and biorelated applications, the QDs should have environmentally benign properties as well as high performances such as high QE and stability. Among various compositions of semiconductor materials, $CuInS_2$ (CIS) can be an alternative emitter for CdSe QDs because the QE of the CIS QDs coated with a ZnS shell is as high as ∼50−60% and the emission color of the CIS QDs can be tuned from green to near-infrared via controlling of size and Cu/In ratio.[4−6] In addition, Cu vacancy-related broad emission is beneficial for blue light-emitting diode (LED)-pumped white LED application because a wide range of visible spectral region can be covered with emission from the CIS QD-converted white LEDs, although only CIS QDs are adapted as converting materials.[6] White LEDs, which are regarded as a next-generation light source, can be fabricated by combining blue LEDs with luminescent materials such as phosphors and QDs.[7−9] When green- and red-emitting QDs are coated onto a blue LED chip, white LEDs with high color rendering index (CRI, R_a) can be fabricated. However, the use of two or three luminescent materials in the LED package may lead to low luminous efficacy due to reabsorption of emission colors.[10−12] In general, full width at half maximums of the emission band of the CdSe and InP QDs are narrow[9,13] and thus, blue LED-pumped yellow-emitting CdSe (or InP) QD-based white LEDs will show a low R_a value and the QDs such as CdSe and InP are not appropriate for the bright white LEDs showing two-band white light. On the contrary, as mentioned above, CIS QDs exhibit broad emission band and they are suitable as a single

Received: January 9, 2015
Accepted: March 10, 2015
Published: March 10, 2015

DOI: 10.1021/acsami.5b00166
ACS Appl. Mater. Interfaces 2015, 7, 6764−6771

color-converting material in the white LED packages. Although, thanks to many efforts, efficient CIS/ZnS core/shell QDs were reported; most CIS/ZnS QDs with high QE over 65% are red- or deep-red-emitting CIS/ZnS or CIS/CdS QDs.[14,15] Some reports indicate that CIS QDs with shorter peak emission wavelengths tend to show lower QEs compared with the CIS QDs with longer peak emission wavelengths.[14,16] Recently, Zhong and co-workers reported green-emissive CIS by Zn addition with a high QE of ∼65% and yellow- and red-emissive CIS QDs (QE ∼ 75%), and they fabricated white LEDs with high CRI values using the green- and red-emissive CIS QDs.[16] The Zn-containing CIS QDs were synthesized to achieve high efficiency and green-emissive CIS QDs. On the other hand, in this study, we used metal−oleate precursors and core/shell/shell structures to synthesize CIS QDs with high QE. Indeed, we successfully synthesized highly efficient yellow-green-emitting CIS/ZnS/ZnS core/shell/shell QDs and fabricated white LEDs showing bright two-band natural white light. The high quality core CIS QDs with QE of ∼30% were first synthesized by using metal−oleate precursors and two separate formation of ZnS shell on the CIS core resulted in yellow-green-emitting CIS/ZnS/ZnS QDs with high QE of 80%. These CIS/ZnS/ZnS QDs were coated on blue LED chips to fabricated white LEDs and bright two-band white light with relatively high CRI value was created from the CIS/ZnS/ZnS QD-converted white LEDs. For application of white LEDs to general illumination, both natural white-emitting white LEDs and warm white-emitting white LEDs are important. Warm white light (lower color temperature) is often used in public area to promote relaxation, whereas natural/cool white light (higher color temperature) is used to enhance concentration in offices.[17] In this study, we would like to fabricate white LEDs emitting white light, which is close to daylight, i.e., natural white light. The luminescent properties of the CIS QDs and optical properties of the natural white-emitting white LEDs were investigated.

2. EXPERIMENTAL SECTION

Materials. To synthesize CIS/ZnS/ZnS core/shell/shell QDs, $CuCl_2{\cdot}2H_2O$ (≥99.99%), $InCl_3{\cdot}4H_2O$ (97%), $Zn(acetate)_2$ (99.99%), dodecanethiol (DDT, ≥98%), 1-octadecene (ODE, technical grade, 90%) were purchased from Sigma-Aldrich and sodium oleate (>97%) was obtained from TCI.

Synthesis of the CIS/ZnS/ZnS QDs. The CIS/ZnS/ZnS core/shell/shell QDs were synthesized via one-pot heating-up route. First, Cu−oleate and In−oleate precursors (Cu:In = 0.25:1) were prepared by adapting the method reported by Hyeon's group.[18] Typically, Cu−oleate was prepared as follows. The $CuCl_2{\cdot}2H_2O$ (0.25 mmol) and Na−oleate (0.5 mmol) were added to the mixed solvents of deionized (DI) water (1.2 mL), ethanol (EtOH, 1.6 mL), and hexane (2.8 mL) in a round-bottom three-neck flask. The mixed solution was heated to 70 °C for 4 h. After completion of the reaction, the upper organic layer was separated and washed for three times with 6 mL of DI water. The In−oleate was prepared with 1 mmol of $InCl_3{\cdot}4H_2O$, Na−oleate (3 mmol), DI water (2.4 mL), EtOH (3.2 mL), and hexane (5.6 mL) using the aforementioned synthetic procedure. A three-neck flask was loaded with 0.25 mmol of Cu−oleate complex and 1 mmol of In−oleate complex, 5 mL of DDT, and 15 mL of ODE. The mixed solution was heated to 100 °C for degassing followed by heating to 230 °C under Ar atmosphere for nucleation and growth of the CIS cores. After 30 min of reaction, 4 mmol of Zn−oleate in mixed solvents of 1 mL of DDT and 5 mL of ODE was added to the reaction flask and then the reaction solution was heated to 250 °C. After 7 h of reaction, for the synthesis of the CIS/ZnS core/shell nanocrystals, 4 mmol of Zn−oleate in the mixture of DDT (1 mL) and ODE (5 mL) was additionally injected into the reaction flask and the reaction solution was maintained at 250 °C for 7 h for the formation of the second ZnS shell. After washing with ethanol (EtOH) several times, the CIS/ZnS/ZnS QDs were dispersed in hexane.

Fabrication of the QD-Converted White LEDs. To fabricate the CIS/ZnS/ZnS QD-converted white LEDs, the CIS/ZnS/ZnS QDs were redispersed in chloroform (optical density ∼ 3.0 at 450 nm), and the solution was mixed with 1.23 g of silicone resin (OE-6630 B, Dow Corning Co.) The concentration of the CIS/ZnS/ZnS QDs was approximately 8.2 wt % in the silicone resin. After the chloroform solvent was removed by heating the mixture at 90 °C for 1 h, a hardener (OE-6630 A) was added to the QD−silicone mixture. The final CIS/ZnS/ZnS QD−silicone resin mixture was coated on a 455 nm blue light-emitting InGaN-based blue LED chip (5.0 × 5.0 mm^2 surface mounting device (SMD) type, Haewon semiconductor, Korea). The blue LED-pumped white LED packages encapsulated with the CIS/ZnS/ZnS−silicone resin was thermally cured at 60 °C for 1 h and then at 150 °C for 1 h, separately.

Characterization. Absorption and photoluminescence (PL) spectra of the CIS-based QD samples were obtained by using a PerkinElmer lambda25 spectrometer and a Hitachi F-7000 spectrophotometer. The size and morphologies of the QDs were investigated by transmission electron microscopy (TEM) by using a Tecnai F20 G^2 transmission electron microscope. The formation of core/shell (CS) and core/shell/shell (CSS) QDs were investigated by energy dispersive X-ray spectroscopy (EDS) using the Tecnai F20 G^2 equipped with EDAX EDS spectrometer PV9761. The CIS core (C), CIS/ZnS CS, and CIS/ZnS/ZnS CSS samples for the EDS measurement were prepared by separately dropping the C, CS, and CSS solutions on the Ni grids coated with amorphous carbon. The chemical compositions of the CIS, CIS/ZnS, and CIS/ZnS/ZnS QDs were investigated by inductively coupled plasma-optical emission spectroscopy (ICP-OES) with a Varian-720ES (Agilent, U.S.A.). The crystal structure of the QDs were analyzed by X-ray diffraction (XRD) using a Bruker D8-Advance operated at 40 kV and 40 mA ($\lambda_{CuK\alpha}$ = 1.5406 Å). The PL QEs of the core, core/shell, and core/shell/shell QDs were obtained by using a quantum efficiency measurement system QE-1100 (Otsuka Electronics co., Japan). The QEs were calculated using the following equation:[19,20]

$$\mathrm{QE} = \frac{N_{em}}{N_{abs}} = \frac{\int \frac{\mathrm{Em}(\lambda)}{hc/\lambda}\mathrm{d}\lambda}{\int \frac{\mathrm{Ex}(\lambda) - \mathrm{Re}(\lambda)}{hc/\lambda}\mathrm{d}\lambda} \quad (1)$$

where, N_{em} is the number of photons for the QD's emission, N_{abs} is the number of the absorbed photons by the QD sample, λ is the wavelength, h is the Planck constant, c is the speed of light, $\mathrm{Em}(\lambda)$ is the intensity of the QD's emission as a function of λ, $\mathrm{Ex}(\lambda)$ is the intensity of the light emitted from the excitation light source as a function of λ, and $\mathrm{Re}(\lambda)$ is reflectance for the QD sample as a function of λ, respectively. The $\mathrm{Ex}(\lambda)$ was measured by using the Spectralon diffusive white standard and empty solvent without the QD sample with the QE-1100 quantum efficiency measurement system.

Optical properties such as electroluminescence (EL) spectrum, luminous efficacy (η_L), correlated color temperature (T_c), Commission Internationale de l'Eclairage (CIE) color coordinates, and CRI values of the fabricated CIS/ZnS/ZnS-converted white LEDs were evaluated under various forward currents of 20−150 mA in an integrating sphere with a diode array rapid analyzer system (PSI Co. Ltd.).

3. RESULTS AND DISCUSSION

It is known that the luminescence from CIS QDs is attributed to radiative transition due to donor−acceptor pair recombination and QE of CIS QDs can be significantly enhanced by the formation of ZnS shell.[3,5,21−23] According to Chen et al., molar ratio of Cu to In influences on the QE of CIS QDs.[21] We also synthesized CIS and CIS/ZnS QDs with varying Cu:In ratios (1:8, 1:4, 1:2, and 1:1) before the formation of the second ZnS

DOI: 10.1021/acsami.5b00166
ACS Appl. Mater. Interfaces 2015, 7, 6764−6771

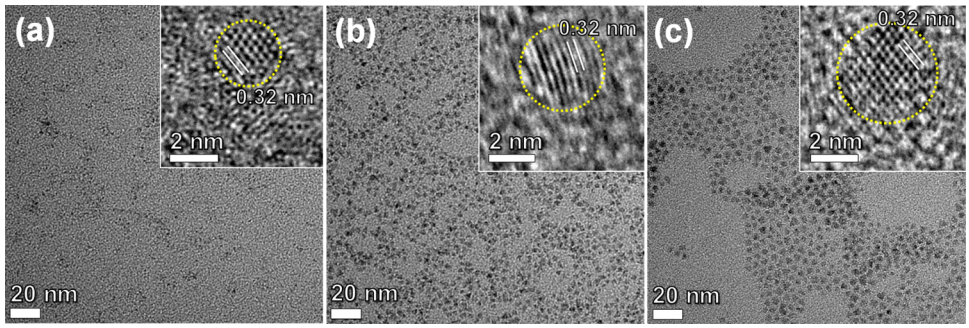

Figure 1. TEM images of (a) CIS core, (b) CIS/ZnS core/shell, and (c) CIS/ZnS/ZnS core/shell/shell QDs, respectively. Insets show corresponding HR-TEM images.

shell on the CIS/ZnS QDs and CIS/ZnS QDs with Cu:In ratio of 1:4 showed the highest PL intensity among the prepared samples (Figure S1 of the Supporting Information). We optimized reaction time to form the first ZnS shell on the CIS core QD. In our experimental conditions, the optimized reaction time was 7 h and longer reactions for the formation of thicker ZnS shells did not result in higher PL intensity, as shown in Figure S2 of the Supporting Information. However, the formation of the second ZnS shell on the CIS/ZnS CS QDs enhanced the PL intensity of the CIS QDs (see below). Thus, we synthesized CIS/ZnS/ZnS QDs in which the ratio of Cu to In was 1:4. For further enhancement of the PL intensity of the CIS QDs, the third ZnS shell was grown on the CIS/ZnS/ZnS CSS QDs. However, the CIS/ZnS/ZnS/ZnS QDs showed similar PL intensity to the CIS/ZnS/ZnS CSS QDs (Figure S3 of the Supporting Information). Figure 1 shows TEM images of $CuInS_2$ core, $CuInS_2$/ZnS CS, and $CuInS_2$/ZnS/ZnS CSS QDs. As the ZnS shell grew, the size of the CIS QDs increased. The particle size increased from 2.5 ± 0.4 nm for the CIS core to 3.5 ± 0.4 nm for the CIS/ZnS core/shell. Finally, the size increased to 4.3 ± 0.4 nm after the second ZnS shell growth on CIS/ZnS QDs. Such a broad size distribution is ascribed to the non-injection-based synthesis and can be partially attributed to continuous release of S^{2-} from DDT molecule throughout the reaction.[6] Although particle size of the CIS core is extremely small, clear lattice fringes are observed in the high resolution TEM (HR-TEM) image of Figure 1a, indicating the high crystallinity of the CIS QDs. The spacing between two adjacent fringes was measured to be 0.32 nm which is accordance with the *d*-spacing between the (112) planes of tetragonal $CuInS_2$ crystals. The CIS/ZnS and CIS/ZnS/ZnS QDs also showed highly clear lattice fringes in the HR-TEM images of Figure 1b,c, respectively. Due to small lattice mismatch (~2%) between $CuInS_2$ and ZnS,[24] although they have different crystal structures, it is postulated that ZnS was epitaxially grown on the CIS core, judging from ambiguity of the interface between the CIS core and ZnS shell in the HR-TEM images. The morphologies (nearly sphere for cores and tetrahedral shape for CS and CSS QDs) of the CIS, CIS/ZnS, and CIS/ZnS/ZnS QDs synthesized with Cu−oleate and In−oleate precursors were similar to those of the previously reported CIS and CIS/ZnS QDs synthesized with CuI and $In(CH_3COO)_3$ precursors.[6,15]

Formation of ZnS shell on the CIS core was directly verified from energy dispersive spectroscopy (EDS) spectra shown in Figure 2. The EDS spectra of the CIS C, CIS/ZnS CS, and CIS/ZnS/ZnS CSS QDs were obtained by using a Tecnai F20 G^2 transmission electron microscope equipped with an EDAX

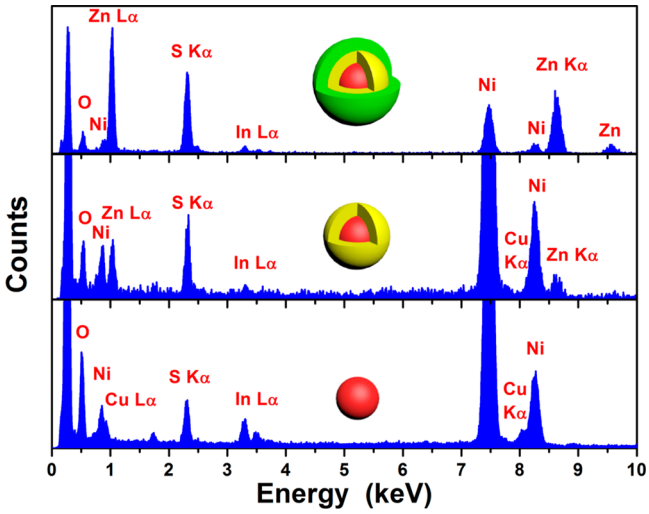

Figure 2. EDS spectra of CIS core (bottom panel), CIS/ZnS core/shell (middle panel), and CIS/ZnS/ZnS core/shell/shell (top panel) QDs.

EDS spectrometer PV9761. The Ni peaks were attributed to the use of the Ni grid coated with carbon to avoid the Cu peaks from the carbon-coated Cu grid, which is frequently used for TEM measurement. In CIS cores, only Cu-, In-, and S-related peaks were observed, whereas in CIS/ZnS and CIS/ZnS/ZnS QDs, Zn-related peaks were observed. Intensities of Cu and In peaks were largely decreased after the growth of the ZnS shell. Moreover, a Cu Lα peak seemed not to be observed due to an intense Zn Lα peak in close proximity of the Cu Lα peak. In addition, the intensity of the Zn Lα peak of CIS/ZnS/ZnS QDs was significantly increased compared with that of CIS/ZnS QDs. In addition to the EDS results, the ICP-OES result confirmed that CIS/ZnS/ZnS QDs were successfully synthesized. For the CIS core, Cu:In:Zn was measured to be 0.05:0.26:0, while Cu:In:Zn ratios were measured to be 0.16:0.68:5.93 and 0.21:0.76:11.52 for the CIS/ZnS and the CIS/ZnS/ZnS QDs, respectively. In the case of the CIS/ZnS/ZnS QDs, the ratio of Cu^+ to In^{3+} was higher than the theoretical value (Cu:In = 1:4) and it may be attributed to the cation exchange between In^{3+} and Zn^{2+} during the reaction. According to Park and Kim,[25] In^{3+} can be exchanged with Zn^{2+} at a high reaction temperature due to the thermodynamic driving force because the ionic radii of In^{3+} and Zn^{2+} are similar to each other (60−62 pm in a four coordinated site) and CIS and ZnS have similar Gibbs formation enthalpies of −221[26] and −206[27] kJ·mol^{-1}. In addition, exchange reactions are allowed in

DOI: 10.1021/acsami.5b00166
ACS Appl. Mater. Interfaces 2015, 7, 6764−6771

particles in nanometer scale regime.[28] Nonetheless, these results confirm that the Cu:In:Zn ratios of the synthesized C, CS, and CSS samples are well consistent with the Cu:In:Zn ratio used in the precursors and the second ZnS shell was well grown on the first ZnS shell.

Figure 3 shows XRD patterns of the CIS, CIS/ZnS, and CIS/ZnS/ZnS QDs. Although molar ratio of Cu to In (1:4) was far

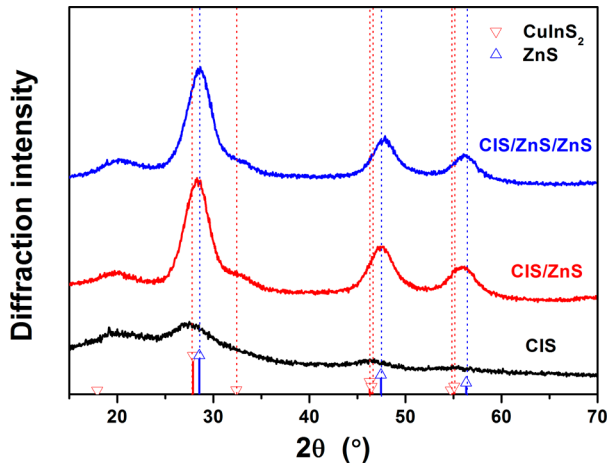

Figure 3. XRD patterns of CIS core, CIS/ZnS core/shell, and CIS/ZnS/ZnS core/shell/shell QDs.

from the stoichiometric ratio (1:1), XRD patterns of the synthesized QD samples were well matched with the literature value of the CIS with a chalcopyrite structure (JCPDS 85-1575). In our Cu deficient synthesis condition, $CuIn_3S_5$ phase might be formed. However, deduction from the $CuIn_3S_5$ phase from the XRD patterns is very difficult because diffraction peak positions of the $CuIn_3S_5$ are close to those of the CIS and the XRD peak of the CIS QDs are broad due to their ultrasmall size. Nonetheless, according to Uehara et al. and Song et al.,[5,6] it was reported that Cu-deficient CIS showed a tetragonal chalcopyrite structure and it is postulated that our CIS QDs also have the chalcopyrite structure. The XRD peak position shifted to a larger 2θ value with the formation of ZnS shell because lattice parameter (a = 5.345 Å) of ZnS with zinc blende structure is smaller than that (a = 5.575 Å) of the CIS with chalcopyrite structure. For instance, the (112) diffraction peak shifted from 27.5° for the CIS cores to 28.6° for the CIS/ZnS/ZnS CSS QDs through 28.3° for the CIS/ZnS CS QDs. This result also indicates that ZnS shell was well grown on the CIS/ZnS CS QDs as well as the CIS core QDs. Particle sizes of the CIS QDs can be calculated by using the Debye−Scherrer equation. The calculated sizes were 2.0, 3.3, and 3.8 nm for CIS C, CIS/ZnS CS, and CIS/ZnS/ZnS CSS, respectively. These values are consistent with the sizes obtained from TEM images.

Figure 4 shows absorption and PL spectra of the CIS C, CIS/ZnS CS, and CIS/ZnS/ZnS CSS QDs. As previously reported from other research groups,[6,14,25] the absorption spectrum was blue-shifted when ZnS shell was formed on the CIS core. The blue shift of the absorption spectrum after ZnS shell formation is attributed to the reduction of the effective core size due to formation of a CIS−ZnS alloy at the interface between the core and the shell[23,29] and cation exchange of Cu^+ and In^{3+} ions by Zn^{2+} ions.[25] The blue shift of the absorption spectrum of the CIS QDs means the increase of band gap energy of the QDs. It led to the blue shift of the PL spectrum of the CIS-based QDs.

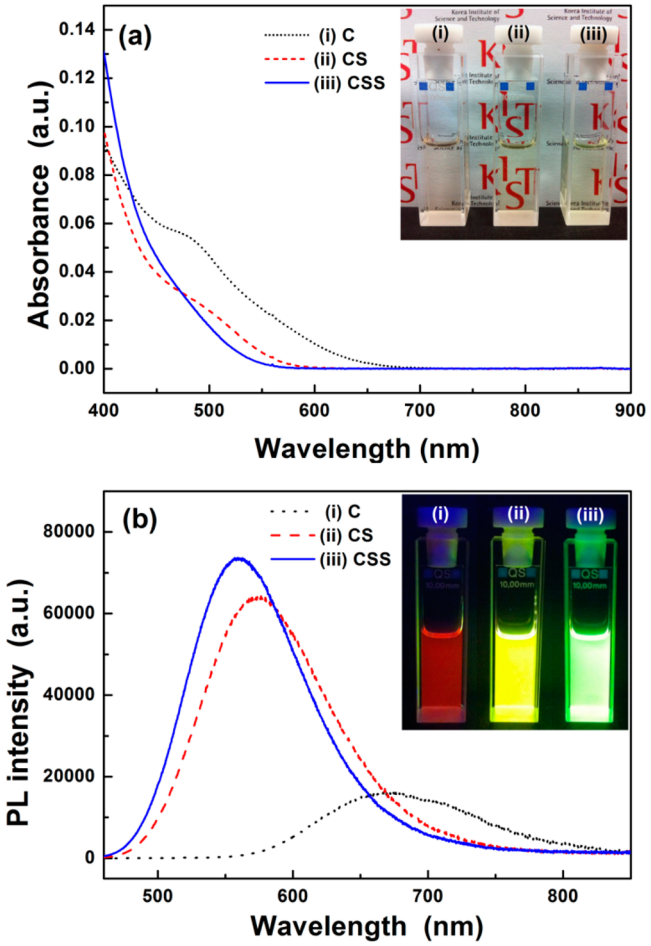

Figure 4. (a) Absorption and (b) PL spectra of (i) CIS core (C), (ii) CIS/ZnS core/shell (CS), and (iii) CIS/ZnS/ZnS core/shell/shell (CSS) QDs. Insets of panels a and b show photographs of CIS, CIS/ZnS, and CIS/ZnS/ZnS solutions taken under room light and UV lamp, respectively.

The peak emission wavelength shifted from 670 nm for the CIS core to 559 nm for the CIS/ZnS/ZnS CSS through 576.4 nm for the CIS/ZnS CS. This blue shift of the PL spectrum is directly verified by emission colors from the CIS (red), CIS/ZnS (yellow), and CIS/ZnS/ZnS (yellow-green) QDs, as shown in Figure 4b inset. The PL QE of the synthesized QDs increased with the formation of ZnS shell. The QEs of red-emitting CIS core, yellow-emitting CIS/ZnS, and yellow-green-emitting CIS/ZnS/ZnS QDs showed 31.7, 76.4, and 80.0% under the excitation of 450 nm, respectively. Although the solvothermally synthesized orange-emitting CIS/ZnS QDs showed the QE of 91%,[30] our yellow-green-emitting CIS/ZnS/ZnS showed higher QE value compared with the QEs (~40−60%) of CIS QDs showing similar color emissions.[16] It is worth noting that to the best of our knowledge, our CIS core showed the highest QEs compared with previously reported CIS cores (mostly below 15%).[15,30−32] This high QE of the CIS core may be attributed to the use of metal−oleate precursors, which allowed long reaction and the formation of core QDs with high crystallinity. In previous reports, reaction time for core synthesis is short (~5−10 min).[6,15] In our synthetic condition, PL intensity of the CIS core was optimized at 30 min reaction. Because the CIS/ZnS synthesized with high quality CIS core showed higher QE than that synthesized from the CIS

DOI: 10.1021/acsami.5b00166
ACS Appl. Mater. Interfaces 2015, 7, 6764−6771

core with low QE,[30] the QE of the CIS/ZnS/ZnS is expected to be enhanced via further synthesis optimization.

Although it was recently reported that the red-emitting CIS/ZnS QDs were additionally incorporated into the white LED package containing the yellow-emitting $Y_3Al_5O_{12}$:Ce phosphor,[33,34] our CIS/ZnS/ZnS QDs are appropriate for single emitter-converted white LEDs due to their broad yellow-green emission with high QE value. In addition to the combination of yellow (yellow-green) light and blue light, the combination of orange light and blue light can also generate white light and orange-emitting CIS/ZnS QDs can be used for the fabrication of white LEDs. However, orange-emitting QDs are suitable for the fabrication of white LED showing warm white light and Song and Yang reported that orange-emitting CIS/ZnS QD-converted LED showed magenta light.[30] In this study, the CIS/ZnS/ZnS CSS QDs were coated onto blue LED chips to fabricate natural white light (or daylight)-emitting white LEDs with high luminous efficacy because the CIS/ZnS/ZnS QDs exhibited higher QE than CIS/ZnS QDs and they showed yellow-green emission in which peak wavelength was shorter than that of CIS/ZnS QDs. To determine the amount of the CIS/ZnS/ZnS QDs in the white LED showing natural white light, the quantity of the CIS/ZnS/ZnS QDs in the silicone resin was adjusted and CIS/ZnS/ZnS QD-converted LEDs containing various amounts of the CIS/ZnS/ZnS QDs were fabricated. The quantity of the CIS/ZnS/ZnS QDs in the silicone resin was slightly increased from low concentration to high concentration to find the appropriate amount for the realization of natural white light from the fabricated white LEDs. As the amount of the CIS/ZnS/ZnS QDs in the LED packages increased, the CIE color coordinates of the CIS/ZnS/ZnS QD-converted LED shifted from blue to yellowish orange region (Figure S4 of the Supporting Information). When the concentration of CIS/ZnS/ZnS QDs in silicone resin was 8.2 wt %, the fabricated white LED generated natural white light, and Figure 5 inset shows an as-fabricated SMD type white LED and its luminescent photograph. The optical properties of the white LED were evaluated at forward bias current of 20 mA. As shown in the photograph of the operating white LEDs in Figure 5, natural white light was generated from the CIS/ZnS/ZnS-converted white LED. It showed the CIE color coordinates of (0.3229, 0.2879) and T_c of 6140 K, and R_a of 73, which is comparable to the R_a value of commercial YAG:Ce-converted white LEDs.[9] After encapsulation with CIS/ZnS/ZnS QD-mixed silicone resin on the blue LED chip, EL intensity of the blue LED largely decreased, while the EL band was newly generated at the yellow spectral region, as shown in Figure 5a. Although integrated area of EL spectrum of the blue LED was larger than that of the CIS/ZnS/ZnS-converted white LED, luminous efficacy of the CIS/ZnS/ZnS QD-converted white LED was much larger than that of the blue LED. Because human eye sensitivity was reflected to the luminous flux unlike the radiant flux,[35] the contribution of the green photons at around 550 nm to the luminous flux is much higher than that of the blue photons at around 450 nm and the fabricated white LED showed high luminous efficacy (η_L = 80.3 lm·W^{-1}). The light conversion efficiency was calculated to be 72.6%, which is comparable the record value (72%) of the LED fabricated with a blue LED and green-emitting CdSe/multishell with the QE of 100%.[36]

The CIE color coordinates of the phosphor-converted white LEDs can be tuned on the straight line connecting the CIE color coordinates of the blue LED and the phosphor.[7]

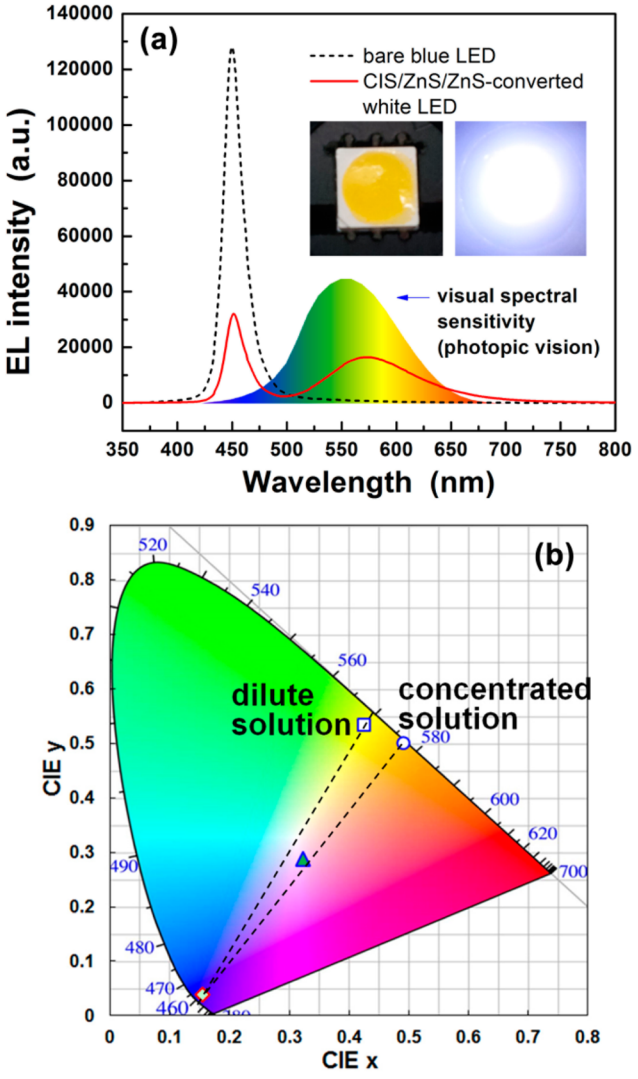

Figure 5. (a) EL spectra of a blue LED (dotted black line) and the CIS/ZnS/ZnS-converted white LED (solid red line) at 20 mA, (b) CIE color coordinates of the CIS/ZnS/ZnS-converted white LED (triangle), blue LED (diamond), dilute CIS/ZnS/ZnS solution (square), and concentrated CIS/ZnS/ZnS solution (circle). Inset of panel a shows the digital camera images of fabricated CIS/ZnS/ZnS-converted white LED under zero bias (left) and forward bias of 20 mA (right).

However, the CIE color coordinates of the fabricated CIS/ZnS/ZnS QD-converted white LED was not located on the line connecting the color coordinates of the CIS/ZnS/ZnS QD-diluted hexane solution and the blue LED (Figure 5b). It is partly attributed to the different concentration of the CIS/ZnS/ZnS QDs in the QD solution and in the fabricated white LED. As described in the Experimental Section, the QD concentration in the silicon resin in the white LED is higher than that in the diluted QD solutions. In this case, the red shift of the PL band of the CIS/ZnS/ZnS QDs was observed. The red shift is ascribed to the local agglomeration of QDs in the silicone resin[37] and a reabsorption of light that emitted from smaller QDs in the ensemble through bigger ones, which have a narrower band gap than smaller ones.[9,38] The local agglomeration of the QDs is due to the difference in the Hildebrand solubility parameters between the silicone and the QD's surfactants.[39] The local agglomeration of the QDs

DOI: 10.1021/acsami.5b00166
ACS Appl. Mater. Interfaces 2015, 7, 6764−6771

increases the efficiency of the energy transfer from smaller QDs to larger QDs, resulting in red shift of the QD's emission.[40,41] In addition, due to the reabsorption effect, the CIS/ZnS/ZnS QDs in the white LEDs showed the red shift of the PL band and simultaneous narrowing of the PL bandwidth. The peak wavelength of the PL band shifted to a longer wavelength from 559 nm for the diluted QD solution to 575 nm for the CIS/ZnS/ZnS QDs in the white LED. The PL bandwidth (91.4 nm) of the CIS/ZnS/ZnS QDs in the white LED was narrower than that (101.9 nm) of the diluted QD solution. When we considered the CIE color coordinates of the concentrated CIS/ZnS/ZnS QD solution, it showed a red shift of the PL band compared with dilute CIS/ZnS/ZnS QD solution due to reabsorption[9] and indeed, its CIE color coordinates shifted from yellow-green to yellowish orange region in the chromaticity diagram. As shown in Figure 5b, the CIE color coordinates of the white LED were found on the line connecting the color coordinates of the concentrated CIS/ZnS/ZnS QD solution and the blue LED.

Optical properties of the two band white light from the QD-converted white LEDs can be easily tailored by adjusting the quantity of the QDs in the silicone encapsulant. When the quantity of the CIS/ZnS/ZnS in the white LED package was slightly increased (The concentration of the QDs in the silicone resin was approximately 9.0 wt %), the fabricated white LED showed a higher η_L of 81.1 lm·W^{-1} but showed a lower R_a of 70. The T_c value decreased from 6140 to 5497 K due to the increase of the ratio of integrated areas of EL spectrum in yellow to blue spectral regions. As shown in Figure 6a, the emission bands of the CIS/ZnS/ZnS QDs increased with increasing applied forward current from 20 to 150 mA, which means that the CIS/ZnS/ZnS QDs exhibit no saturation. However, the CIE color coordinates of the white LED slightly shifted to blue region in the chromaticity diagram with increasing forward current. The blue-shifted color coordinates of the white LED can be explained by thermal quenching effect of the CIS-based QDs at high forward current. As shown in Figures 6a and S5 of the Supporting Information, luminescence saturation of the CIS/ZnS/ZnS QDs in the white LEDs was not observed against the increase of the forward current. When the forward current increases, junction temperature of the LED chip in the white LEDs rises.[42,43] The higher junction temperature raises the temperature around QDs in the silicone encapsulant. It results in the thermal quenching of the CIS/ZnS/ZnS QDs' luminescence because thermal quenching is strong for these QDs.[33] Consistently, light conversion efficiency slightly decreased from 72% at 20 mA to 64% at 150 mA, as shown in Figure 6b. On the contrary, luminous efficacy decreased significantly (81.1 lm·W^{-1} at 20 mA → 37.5 lm·W^{-1} at 150 mA), which is attributed to the decreased of the internal quantum efficiency (IQE) of the nitride-based blue LEDs with increasing forward current.[6,44,45] Except for lowered luminous efficacy due to the drop of the IQE of the blue LED, other white light properties of the white LEDs were quite stable against the increase of forward current from 20 to 150 mA. The CIE color coordinates of the white LED varied from (0.3220, 0.2997) at 20 mA to (0.3207, 0.2867) at 150 mA. The R_a increased from 70 to 72 and the T_c increased from 5497 to 6375 K, respectively, under the increase of forward current from 20 to 150 mA. These results show that white light generated from the CIS/ZnS/ZnS-converted white LED has high stability against the increase of forward bias current.

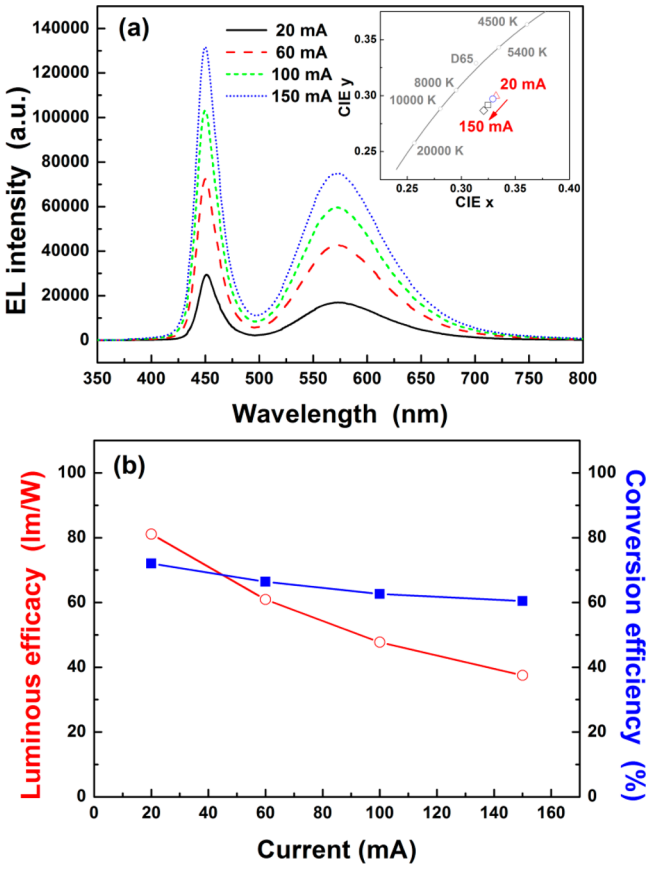

Figure 6. (a) EL spectra and (b) luminous efficacies and light conversion efficiencies of the CIS/ZnS/ZnS-converted white LED at various forward currents of 20, 60, 100, and 150 mA. Inset of panel a shows variation of the CIE color coordinates of the white LED at various forward currents of 20 mA (triangle), 60 mA (circle), 100 mA (square), and 150 mA (diamond).

4. CONCLUSION

In this study, highly bright yellow-green-emitting CIS/ZnS/ZnS CSS QDs were successfully synthesized by using metal−oleate precursors and the separate injection of Zn and S precursors to the reaction solution containing the CIS cores. The XRD, TEM, EDS, and ICP analyses confirmed the synthesis of the CSS structure. With the formation of the first and the second ZnS shells, the peak of the PL band shifted to a shorter wavelength (670 nm → 559 nm) and the QE significantly increased from 31.7% for the core QDs to 80.0% for the CSS QDs. Thanks to the use of the metal−oleate precursors, highly efficient CIS cores with the QE of 31.7% were obtained, and they can be a foundation for eminent yellow- or green-emitting CS or CSS QDs having extremely high QE values over 90% for further synthesis optimization. When the CIS/ZnS/ZnS CSS QDs were coated on the blue LED, bright white LEDs were fabricated. The white LED showed bright natural white light [(CIE x, CIE y) = (0.3229, 0.2879), η_L = 80.3 lm·W^{-1}, T_c = 6140 K, and R_a = 73]. The fabricated white LED was also relatively stable against the increase of forward current. It indicates that the CIS/ZnS/ZnS QD is a promising material applicable to blue LED-pumped white LEDs showing bright two-band white light.

DOI: 10.1021/acsami.5b00166
ACS Appl. Mater. Interfaces 2015, 7, 6764−6771

■ ASSOCIATED CONTENT

Supporting Information

Luminescence images and PL spectra of $CuInS_2$ core and $CuInS_2$/ZnS core/shell QD solutions with different Cu:In ratios, PL spectra of $CuInS_2$/ZnS core/shell QDs with varying shell reaction time, PL spectra of $CuInS_2$/ZnS/ZnS/ZnS core/shell/shell/shell QDs, photographs and color coordinates of $CuInS_2$/ZnS/ZnS QD-converted LEDs, and emission intensities of the CIS/ZnS/ZnS QDs and blue LED chip in the white LEDs with increasing forward current. This material is available free of charge via the Internet at http://pubs.acs.org.

■ AUTHOR INFORMATION

Corresponding Author

*H. S. Jang. Tel: +82-2-958-5263. Fax: +82-2-958-5599. E-mail: msekorea@kist.re.kr.

Author Contributions

‖These authors contributed equally to this work.

Notes

The authors declare no competing financial interest.

■ ACKNOWLEDGMENTS

This work is supported by the Future Key Technology Program (2E25371) and Dream Project (2V03410) funded by the Korea Institute of Science and Technology and the Pioneer Research Center Program through the National Research Foundation of Korea funded by the Ministry of Science, ICT & Future Planning (NRF-2013M3C1A3065040).

■ REFERENCES

(1) Murray, C. B.; Norris, D. J.; Bawendi, M. G. Synthesis and Characterization of Nearly Monodisperse CdE (E = Sulfur, Selenium, Tellurium) Semiconductor Nanocrystallites. *J. Am. Chem. Soc.* **1993**, *115*, 8706−8715.

(2) Dabbousi, B. O.; Rodriguez-Viejo, J.; Mikulec, F. V.; Heine, J. R.; Mattoussi, H.; Ober, R.; Jensen, K. F.; Bawendi, M. G. (CdSe)ZnS Core-Shell Quantum Dots: Synthesis and Characterization of a Size Series of Highly Luminescent Nanocrystallites. *J. Phys. Chem. B* **1997**, *101*, 9463−9475.

(3) Nam, D.-E.; Song, W.-S.; Yang, H. Noninjection, One-Pot Synthesis of Cu-Deficient $CuInS_2$/ZnS Core/Shell Quantum Dots and Their Fluorescent Properties. *J. Colloid Interface Sci.* **2011**, *361*, 491−496.

(4) Xie, R.; Rutherford, M.; Peng, X. Formation of High-Quality I−III−VI Semiconductor Nanocrystals by Tuning Relative Reactivity of Cationic Precursors. *J. Am. Chem. Soc.* **2009**, *131*, 5691−5697.

(5) Uehara, M.; Watanabe, K.; Tajiri, Y.; Nakamura, H.; Maeda, H. Synthesis of $CuInS_2$ Fluorescent Nanocrystals and Enhancement of Fluorescence by Controlling Crystal Defect. *J. Chem. Phys.* **2008**, *129*, 134709.

(6) Song, W.-S.; Yang, H. Efficient White-Light-Emitting Diodes Fabricated from Highly Fluorescent Copper Indium Sulfide Core/Shell Quantum Dots. *Chem. Mater.* **2012**, *24*, 1961−1967.

(7) Jang, H. S.; Won, Y.-H.; Jeon, D. Y. Improvement of Electroluminescent Property of Blue LED Coated with Highly Luminescent Yellow-Emitting Phosphors. *Appl. Phys. B: Lasers Opt.* **2009**, *95*, 715−720.

(8) Jang, H. S.; Kwon, B.-H.; Yang, H.; Jeon, D. Y. Bright Three-Band White Light Generated from CdSe/ZnSe Quantum Dot-Assisted $Sr_3SiO_5:Ce^{3+}$, Li^+-based White Light-Emitting Diode with High Color Rendering Index. *Appl. Phys. Lett.* **2009**, *95*, 161901.

(9) Jang, H. S.; Yang, H.; Kim, S. W.; Han, J. Y.; Lee, S.-G.; Jeon, D. Y. White Light-Emitting Diodes with Excellent Color Rendering Based on Organically Capped CdSe Quantum Dots and $Sr_3SiO_5:Ce^{3+},Li^+$ Phosphors. *Adv. Mater.* **2008**, *20*, 2696−2702.

(10) Won, Y.-H.; Jang, H. S.; Cho, K. W.; Song, Y. S.; Leon, D. Y.; Kwon, H. K. Effect of Phosphor Geometry on The Luminous Efficiency of High-Power White Light-Emitting Diodes with Excellent Color Rendering Property. *Opt. Lett.* **2009**, *34*, 1−3.

(11) Won, Y.-H.; Jang, H. S.; Im, W. B.; Jeon, D. Y.; Lee, J. S. Tunable Full-Color-Emitting $La_{0.827}Al_{11.9}O_{19.09}:Eu^{2+},Mn^{2+}$ Phosphor for Application to Warm White-Light-Emitting Diodes. *Appl. Phys. Lett.* **2006**, *89*, 231909.

(12) Kim, J. S.; Jeon, P. E.; Choi, J. C.; Park, H. L.; Mho, S. I.; Kim, G. C. Warm-White-Light Emitting Diode Utilizing a Single-Phase Full-Color $Ba_3MgSi_2O_8:Eu^{2+}$, Mn^{2+} Phosphor. *Appl. Phys. Lett.* **2004**, *84*, 2931−2933.

(13) Lim, K.; Jang, H. S.; Woo, K. Synthesis of Blue Emitting InP/ZnS Quantum Dots through Control of Competition between Etching and Growth. *Nanotechnology* **2012**, *23*, 485609.

(14) Deng, D.; Chen, Y.; Cao, J.; Tian, J.; Qian, Z.; Achilefu, S.; Gu, Y. High-Quality $CuInS_2$/ZnS Quantum Dots for in Vitro and in Vivo Bioimaging. *Chem. Mater.* **2012**, *24*, 3029−3037.

(15) Li, L.; Pandey, A.; Werder, D. J.; Khanal, B. P.; Pietryga, J. M.; Klimov, V. I. Efficient Synthesis of Highly Luminescent Copper Indium Sulfide-based Core/Shell Nanocrystals with Surprisingly Long-Lived Emission. *J. Am. Chem. Soc.* **2011**, *133*, 1176−1179.

(16) Chen, B.; Zhong, H.; Wang, M.; Liu, R.; Zou, B. Integration of $CuInS_2$-based Nanocrystals for High Efficiency and High Colour Rendering White Light-Emitting Diodes. *Nanoscale* **2013**, *5*, 3514−3519.

(17) Paschotta, R. *Encyclopedia of Laser Physics and Technology*; Wiley-VCH: Weinheim, Germany, 2008.

(18) Park, J.; An, K. J.; Hwang, Y.; Park, J.-G.; Noh, H.-J.; Kim, J.-Y.; Park, J.-H.; Hwang, N.-M.; Hyeon, T. Ultra-Large-Scale Syntheses of Monodisperse Nanocrystals. *Nat. Mater.* **2004**, *3*, 891−895.

(19) Kamiyama, Y.; Hiroshima, T.; Isobe, T.; Koizuka, T.; Takashima, S. Photostability of YAG:Ce^{3+} Nanophosphors Synthesized by Glycothermal Method. *J. Electrochem. Soc.* **2010**, *157*, J149−J154.

(20) Jang, H. S.; Kim, H. Y.; Kim, Y.-S.; Lee, H. M.; Jeon, D. Y. Yellow-Emitting γ-$Ca_2SiO_4:Ce^{3+},Li^+$ Phosphor for Solid-Sate Lighting: Luminescent Properties, Electronic Structure, and White Light-Emitting Diode Application. *Opt. Express* **2012**, *20*, 2761−2771.

(21) Chen, B.; Zhong, H.; Zhang, W.; Tan, Z.; Li, Y.; Yu, C.; Zhai, T.; Bando, Y.; Yang, S.; Zou, B. Highly Emissive and Color-Tunable $CuInS_2$-based Colloidal Semiconductor Nanocrystals: Off-Stoichiometry Effects and Improved Electroluminescence Performance. *Adv. Funct. Mater.* **2012**, *22*, 2081−2088.

(22) Zhong, H.; Bai, Z.; Zou, B. Tuning the Luminescence Properties of Colloidal I−III−VI Semiconductor Nanocrystals for Optoelectronics and Biotechnology Applications. *J. Phys. Chem. Lett.* **2012**, *3*, 3167−3175.

(23) Kim, H.; Han, J. Y.; Kang, D. S.; Kim, S. W.; Jang, D. S.; Suh, M.; Kirakosyan, A.; Jeon, D. Y. Characteristics of $CuInS_2$/ZnS Quantum Dots and Its Application on LED. *J. Cryst. Growth* **2011**, *326*, 90−93.

(24) Pons, T.; Pic, E.; Lequeux, N.; Cassette, E.; Bezdetnaya, L.; Guillemin, F.; Marchal, F.; Dubertret, B. Cadmium-Free $CuInS_2$/ZnS Quantum Dots for Sentinel Lymph Node Imaging with Reduced Toxicity. *ACS Nano* **2010**, *4*, 2531−2538.

(25) Park, J.; Kim, S.-W. $CuInS_2$/ZnS Core/Shell Quantum Dots by Cation Exchange and Their Blue-Shifted Photoluminescence. *J. Mater. Chem.* **2011**, *21*, 3745−3750.

(26) Wiedemeier, H.; Santandrea, R. Mass Spectrometric Studies of the Decomposition and the Heat of Formation of $CuInS_2$(s). *Z. Anorg. Allg. Chem.* **1983**, *497*, 105−118.

(27) Deore, S.; Navrotsky, A. Oxide Melt Solution Calorimetry of Sulfides: Enthalpy of Formation of Sphalerite, Galena, Greenockite, and Hawleyite. *Am. Mineral.* **2006**, *91*, 400−403.

(28) Son, D. H.; Hughes, S. M.; Yin, Y.; Alivisatos, A. P. Cation Exchange Reactions in Ionic Nanocrystals. *Science* **2004**, *306*, 1009−1012.

DOI: 10.1021/acsami.5b00166
ACS Appl. Mater. Interfaces 2015, 7, 6764−6771

(29) Nam, D.-E.; Song, W.-S.; Yang, H. Facile, Air-Insensitive Solvothermal Synthesis of Emission-Tunable $CuInS_2$/ZnS Quantum Dots with High Quantum Yields. *J. Mater. Chem.* **2011**, *21*, 18220−18226.
(30) Song, W.-S.; Yang, H. Fabrication of White Light-Emitting Diodes Based on Solvothermally Synthesized Copper Indium Sulfide Quantum Dots as Color Converters. *Appl. Phys. Lett.* **2012**, *100*, 183104.
(31) Wang, M.; Liu, X.; Cao, C.; Wang, L. Highly Luminescent $CuInS_2$-ZnS Nanocrystals: Achieving Phase Transfer and Nuclear Homing Property Simultaneously through Simple TTAB Modification. *J. Mater. Chem.* **2012**, *22*, 21979−21986.
(32) Zhang, W.; Zhong, X. Facile Synthesis of ZnS−$CuInS_2$-Alloyed Nanocrystals for a Color-Tunable Fluorchrome and Photocatalyst. *Inorg. Chem.* **2011**, *50*, 4065−4072.
(33) Aboulaich, A.; Michalska, M.; Schneider, R.; Potdevin, A.; Deschamps, J.; Deloncle, R.; Chadeyron, G.; Mahiou, R. Ce-Doped YAG Nanophosphor and Red Emitting $CuInS_2$/ZnS Core/Shell Quantum Dots for Warm White Light-Emitting Diode with High Color Rendering Index. *ACS Appl. Mater. Interfaces* **2014**, *6*, 252−258.
(34) Sohn, I. S.; Unithrattil, S.; Im, W. B. Stacked Quantum Dot Embedded Silica Film on a Phosphor Plate for Superior Performance of White Light-Emitting Diodes. *ACS Appl. Mater. Interfaces* **2014**, *6*, 5744−5748.
(35) Wyszecki, G.; Stiles, W. S. *Color Science: Concepts and Methods, Quantatative Data and Formulae*, 2nd ed.; John Wiley & Sons, Inc.: New York, 1982.
(36) Jun, S.; Jang, E. Bright and Stable Alloy Core/Multishell Quantum Dots. *Angew. Chem., Int. Ed.* **2013**, *52*, 679−682.
(37) Kim, H.; Kwon, B.-H.; Suh, M.; Kang, D. S.; Kim, Y.; Jeon, D. Y. Degradation Characteristics of Red Light-Emitting $CuInS_2$/ZnS Quantum Dots as a Wavelength Converter for LEDs. *Electrochem. Solid-State Lett.* **2011**, *14*, K55−K57.
(38) Manna, L.; Scher, E. C.; Li, L.-S.; Alivisatos, A. P. Epitaxial Growth and Photochemical Annealing of Graded CdS/ZnS Shells on Colloidal CdSe Nanorods. *J. Am. Chem. Soc.* **2002**, *124*, 7136−7145.
(39) Schreuder, M. A.; Gosnell, J. D.; Smith, N. J.; Warnement, M. R.; Weiss, S. M.; Rosenthal, S. J. Encapsulated White-Light CdSe Nanocrystals as Nanophosphors for Solid-State Lighting. *J. Mater. Chem.* **2008**, *18*, 970−975.
(40) Crooker, S. A.; Hollingsworth, J. A.; Tretiak, S.; Klimov, V. I. Spectrally Resolved Dynamics of Energy Transfer in Quantum-Dot Assemblies: Towards Engineered Energy Flows in Artificial Materials. *Phys. Rev. Lett.* **2002**, *89*, 186802.
(41) Wuister, S. F.; Swart, I.; van Driel, F.; Hickey, S. G.; de Mello Donegá, C. Highly Luminescent Water-Soluble CdTe Quantum Dots. *Nano Lett.* **2003**, *3*, 503−507.
(42) Xi, Y.; Schubert, E. F. Junction−Temperature Measurement in GaN Ultraviolet Light-Emitting Diodes Using Diode Forward Voltage Method. *Appl. Phys. Lett.* **2004**, *85*, 2163−2165.
(43) Jiang, F.; Liu, W.; Li, Y.; Fang, W.; Mo, C.; Zhou, M.; Liu, H. Research on the Junction-Temperature Characteristic of GaN Light-Emitting Diodes on Si Substrate. *J. Lumin.* **2007**, *122*−*123*, 693−695.
(44) Piprek, J. Efficiency Droop in Nitride-based Light-Emitting Diodes. *Phys. Status Solid A* **2010**, *207*, 2217−2225.
(45) Laubsch, A.; Sabathil, M.; Bergbauer, W.; Strassburg, M.; Lugauer, H.; Peter, M.; Lutgen, S.; Linder, N.; Streubel, K.; Hader, J.; Moloney, J. V.; Pasenow, B.; Koch, S. W. On the Origin of IQE-'droop' in InGaN LEDs. *Phys. Status Solid C* **2009**, *6*, S913−S916.

DOI: 10.1021/acsami.5b00166
ACS Appl. Mater. Interfaces 2015, 7, 6764−6771